DOKUZ EYLÜL UNIVERSITY

GRADUATE SCHOOL OF NATURAL AND APPLIED SCIENCES

EVALUATION OF BLEG AND -80 MESH STREAM SEDIMENT ASSAY RESULTS OBTAINED FROM TURKEY UTM (UNIVERSAL TRANSVERSAL MERKATOR) 36 ZONE BY PARAMETRIC AND NON-PARAMETRIC STATISTICAL METHODS

by

Simay KOÇKAR

October, 2021

İZMİR

EVALUATION OF BLEG AND -80 MESH STREAM SEDIMENT ASSAY RESULTS OBTAINED FROM TURKEY UTM (UNVERSAL TRANSVERSAL MERKATOR) 36 ZONE BY PARAMETRIC AND NON-PARAMETRIC STATISTICAL METHODS

A Thesis Submitted to the
Graduate School of Natural and Applied Sciences of Dokuz Eylül University In Partial Fulfillment of the Requirements for the Degree of Master in Geological Engineering, Economical Geology Program

by
Simay KOÇKAR

October, 2021
İzmir

M.Sc THESIS EXAMINATION RESULT FORM

We have read the thesis entitled **"EVALUATION OF BLEG AND -80 MESH STREAM SEDIMENT ASSAY RESULTS OBTAINED FROM TURKEY UTM (UNVERSAL TRANSVERSAL MERKATOR) 36 ZONE BY PARAMETRIC AND NON-PARAMETRIC STATISTICAL METHODS"** completed by **SİMAY KOÇKAR** under supervision of **ASSIST. PROF. DR. FATMA NURAN SÖNMEZ** and we certify that in our opinion it is fully adequate, in scope and in quality, as a thesis for the degree of Master of Science.

Assist. Prof. Dr. Fatma Nuran Sönmez

Supervisor

Prof. Dr. Hülya İnaner

(Jury Member)

Assist. Prof. Dr. Hüseyin Sendir

(Jury Member)

Prof.Dr. Özgür ÖZÇELİK

Director

Graduate School of Natural and Applied Sciences

ACKNOWLEDGMENTS

This research would not have been possible without the exceptional support of my supervisor Assist. Prof. Dr. Fatma Nuran SÖNMEZ. Her hard work to enlighten my path when I lost my way, kept me going through this phase of my life. Even though he is already retired Prof. Dr. Hüseyin YILMAZ, his exertion on this research would be unfeasible to ignore. His knowledge and his experience taught me very much. He has the patience to answer all my questions and in this way I have got the chance to cover up my lack of knowledge. I am also very thankful for the support of my colleagues; Research Assistant Ayça YILDIRIM, Research Assistant Anıl KÜÇÜKSÜMBÜL and M.Sc. Metehan ULUĞTEKİN, during this research they have been splendid team mates. They made the university feel like home. Finally, I want to thank my family; my father Yusuf Çetin KOÇKAR, my mother Zuhal KOÇKAR, my brother Kutay KOÇKAR, my sister-like Research Assistant Meltem MUTLUTÜRK and my fiancé Ali ÖZTÜRK for supporting me both mentally and physically and for encouraging me through the end of this journey.

Simay KOÇKAR

EVALUATION OF BLEG AND -80 MESH STREAM SEDIMENT ASSAY RESULTS OBTAINED FROM TURKEY UTM (UNIVERSAL TRANSVERSAL MERKATOR) 36 ZONE BY PARAMETRIC AND NON-PARAMETRIC STATISTICAL METHODS

ABSTRACT

As expressed by numerous researchers, fine-grained stream sediment sampling occupies its first place for geochemical sampling environment at ore deposit discovery surveys in most part of the earth. In gold and silver investigation, the analysis of Bulk Leach Extractable Gold (BLEG) settles in the first place whereas acid-extractable gold in minus eighty mesh stream sediment fraction has been commonly used during follow up of the BLEG results.

The Eskisehir-Sivrihisar region in Western Turkey includes several orogenic type mineral deposits including gold-bearing quartz vein systems. Using a geochemical database generated through company's exploration campaigns, this research compares the capability of conventional statistical techniques Mean + 2STD, Median + 2MAD) and principal component analysis (PCA), with number-concentration (N-S) fractal and concentration-area (C-A) methods and singularity index (SI) method to differentiate anomalous and background gold distributions or define areas with geochemical signals related to mineralization (given singularity index mapping does not define threshold values).

Gold mineralizations discovered in the area of interest in the past were re-uncovered by BLEG gold stream sediment anomalies, which have used robust singularity indices with C-A and N-S multifractal modeling and PCA. Eighty-five percent of the gold deposits were defined using either BLEG silver or less than one hundred eighty micrometers stream sediment silver data. Conventional approaches to anomaly detection for the BLEG and less than one hundred eighty micrometers stream sediment data failed to detect a number of significant deposits, including some in the vicinity of Sivrihisar.

Keywords: Singularity mapping, concentration-area, number-size, principal component analysis, multi fractal models, Eskisehir-Sivrihisar area

TÜRKİYE 36. EVRENSEL ENLEM ZONUNDAN ELDE EDİLEN BLEG VE -80 MESH DERE TORTULU ÖRNEĞİ ANALİZ SONUÇLARININ PARAMETRİK VE PARAMETRİK OLMAYAN İSTATİSTİKSEL YÖNTEMLERLE DEĞERLENDİRİLMESİ

ÖZ

Çok sayıda araştırmacının dile getirdiği gibi ince taneli dere tortulu örneklemesi, iyi gelişmiş drenaj sistemlerinin bulunduğu bölgelerde, bölgesel mineral araştırmaları sırasında ilk olarak yapılan jeokimyasal örnekleme çalışmasıdır. Altın ve gümüş araştırmalarında, yaygın olarak yıkanmış ve ekstrakte edilebilir kütlesel altın çözündürme (BLEG) analizi ilk sırada kullanılırken, bu BLEG analizi sonuçlarını takip etme amacı ile asitle ekstrakte edilebilir altın eksi seksen mesh dere tortulu analizleri kullanılır.

Türkiye’nin batısındaki Eskişehir-Sivrihisar bölgesi, altın içeren kuvars damar sistemleri de dahil olmak üzere birçok orojenik tip maden yatakları içerir. Bir şirketin araştırma kampanyaları sayesinde elde edilen jeokimyasal veri tabanı kullanılarak yapılan bu araştırmada, anomalileri ve arka planda kalan altın dağılımları veya mineralizasyonla ilgili jeokimyasal olarak sinyal veren alanların teşhis edilmesi için , geleneksel istatistiksel çalışma metotları (Q-Q, ortalama + 2STD, medyan + 2MAD gibi çalışmalar) ile konsantrasyon alanı (C-A), sayı-boyut (N-S) fraktal yöntemleri ve tekillik indeksi (SI) yöntemiyle, temel bileşen analizini (PCA) karşılaştırılmıştır (verilen tekillik indeksi eşlemesi, eşik değerlerini tanımlamaz).

Geçmişte ilgili alanda keşfedilen altın cevherleşmeleri, güçlü tekillik indeksleri kullanan C-A, N-S multifraktal modelleme ve PCA ile BLEG altın dere tortulu anomalileriyle yeniden ortaya konulmuştur. Altın yataklarının yüzde seksen beşi, BLEG-gümüşü veya yüz seksen mikrometreden az dere tortulu gümüşü verileri kullanılarak tanımlanmıştır. BLEG ve yüz seksen mikrometreden az dere tortulu verilerinin anomali tespiti için kullanılan geleneksel yöntemlerin Sivrihisar yöresi de

dahil olmak üzere bazı önemli yatakların bulunması konusunda başarısız olduğu görülmüştür.

Anahtar kelimeler: Tekillik haritalama, konsantrasyon-alan, sayı-konsantrasyon, temel bileşenler analizi, multifraktal modelleme, Eskişehir-Sivrihisar bölgesi

CONTENTS

LIST OF FIGURES

Page

LIST OF TABLES

Page

CHAPTER 1
INTRODUCTION

Detection of significant mineralization-associated geochemical patterns or anomalies is of great importance in exploring for ore deposits. Several statistical methods have been investigated for generating robust geochemical anomaly maps and models from exploration geochemical data. These include conventional parametric and non-parametric methods (Govett et al., 1975; Sinclair, 1991; Tukey, 1977), and alternative techniques that are not dependent on data distribution types or affected by the presence of outlying populations including fractal modelling (Afzal et al., 2011; Cheng, 1999; Mandelbrot, 1983; Sadeghi et al., 2015; Zuo, 2011) and basin analysis (Bonham-Carter et al., 1987; Carranza, 2010). In recent years there has been a move to the latter as a more robust approach to the recognition of significant geochemical anomalies (Carranza, 2010a, b; Cheng et al., 1994; Grunsky, 2007, 2010; Zuo and Wang, 2016). Linked to this is the need to consider spatial patterns and other processes that can lead to complexity in defining geochemically anomalous behavior (Parsa et al., 2017a; Yilmaz et al., 2019; Zuo et al., 2012).

EDA methods are not as robust as fractal modelling in the case of sparse geochemical data. Most EDA methods ignore spatial relations between geochemical data whereas fractal modelling may be designed so as to consider spatial relationships between regolith geochemistry and known mineral deposits (Agterberg et al., 1990).

Fractal modelling uses the complete geochemical data set without the necessity of transformations to meet assumptions about data distribution and effects of outliers (He et al., 2013; Luz et al., 2014). Fractal modelling is predicted on power-law distribution, which means that some statistical characteristics of the data are invariant (self-similar) at different scales (Mandelbrot, 1983; Shen & Cohen 2005). Fractal models that have obtained a noteworthy application in delineating geochemical anomalies are the concentration-area (C-A) and number-size (N-S) , singularity indexes (SI) and concentration-volume (C-V) (Afzal et al., 2010; Cheng et al., 1996, 1999, 2000; Cheng, 2007; Mandelbrot, 1983;). Shuguang et al. (2015) has classified fractal or multifractal approaches employed in geochemical anomaly definition into hard- and soft-threshold techniques. The hard-threshold group includes N-S and C-A fractal models with clear-cut thresholds to define population breaks and identify anomalies but fails to identify more subtle changes in fractal behavior typical of complicated or composite geological environments (Zuo et al., 2013). The soft-threshold methods include S-A and SI multifractal techniques. These filtering methods improve the reliability in setting thresholds for geochemically anomalous populations but are not able to determine sill for separating geochem populations (Zuo & Wang, 2016). Thus, geochemical signatures generated by singularity mapping procedures essentially have needed additional calibration of geochemical values to adjust for potential dilution effects following the concepts of Hawkes (1976). For stream sediment geochemistry sediment dilution in drainage must also be taken into account as a potential factor in setting thresholds to background Au distributions. The typical approach is to use catchment area weighting. This study compares the results of selected conventional and fractal methods to define anomalous catchments based on both raw and catchment-weighted BLEG Au and Ag values. Verification of the results attained can be employed utilizing geochemical properties of already discovered gold deposits and prospects along with the rock chip samples in the area.

CHAPTER 2
STUDY AREA AND DATA

2.1 Regional Geology and Tectonic Settings

The investigated area of ~2,660 km^2 is located in the Eskisehir region of Western Anatolia. It is underlain by three significant ore-hosting stratigraphic units (Figure 2.1). These are: a) the Precambrian to Lower Paleozoic, undifferentiated high-grade unit, consisting of gneiss, metagranite, schist, amphibolite and marble, which are cut by Upper Paleozoic granitoids; b) the Triassic Karakaya Complex containing schists at low-grade and metasedimentary units, and metamorphosed volcanic inter-beddings (Altiner et al., 1991; Okay et al., 1996) and c) Cretaceous ophiolites or accretionary meta-clastic rocks intruded by Cenozoic magmatic rocks (Okay and Satır, 2000; Yilmaz, 2003). The Karakaya Complex contains metamorphosed mafic rocks, low-grade shists and marbles.

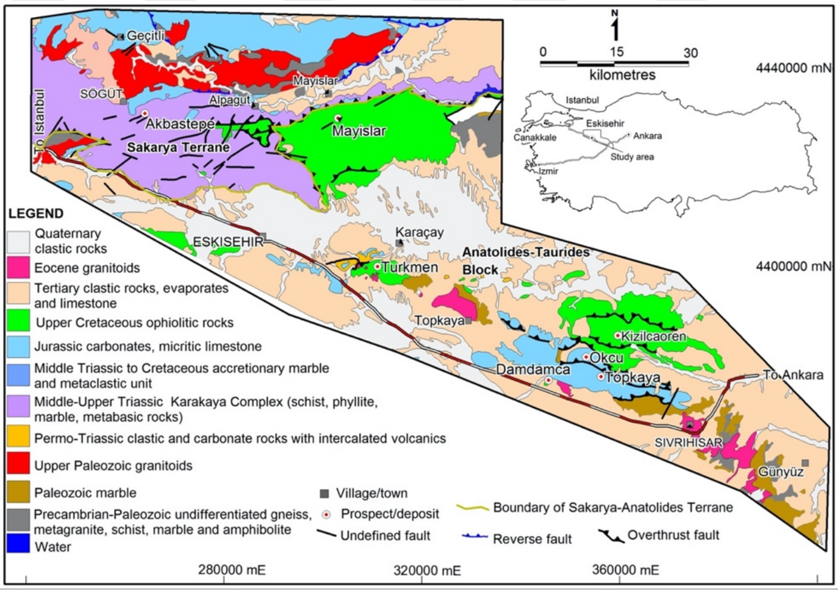

Figure 2.1 Simplified geological map of the Karakaya (After Okay et al., 1996, Okay and Satır, 2000, MTA, 2002, Yilmaz, 2003, and this study)

2.2 Local Geology and Mineralization

The Karakaya Complex include the probable orogenic Akbastepe Au-As-Sb-W mineralization (SE of Sogut; MTA, 1965, 1970; Yilmaz, 2003), as well as the epithermal-style Damdamca and Topkaya Au-Ag deposits to the NW of Sivrihisar, and the Mayıslar and Türkmen mineralizations (Table 2.1). In the Akbaştepe mineralization, Au occurs in quartz veins, with peak grades of 20 g/t Au over a 220 m strike length and 2 m width (Eurogold Company report, 1996) in low- grade schists and marbles. The Damdamca and Topkaya gold-silver-arsenic mineralizations have a combined indicated resource of 1.450 Mt at 4.06 g/t Au, and 1.950 Mt resource with an average ore grade of 4.9 g/t Au (Koza Gold, 2013). The Damdamca deposit occurs in a serpentinite block. Topkaya deposit is hosted in marble and meta-clastic rocks. Both of these deposits are hosted in the footwall of a south-verging thrust (Yilmaz, 2003).

The sub-economic Mayislar Cu-Pb-Zn-As-Mo occurs in Eocene andesite and Cretaceous ophiolites (Parlak and Sayili, 2012). In the mineralization, altered andesite with tourmaline are crossed by several silica and calcite veinlets.

The Türkmen mineralization is hosted by Upper Cretaceous ophiolites. In this ophiolites there are altered serpentinite that hosting silica stockwork that contains sfalerite, galena and pyrite, and minor chalcopyrite and arsenopyrite (Eurogold, 1996; Yilmaz, 2003). An Fe-oxide altered silica cap overlies the intrusive rocks. The Turkmen deposit has a similarity to porphyry stock-related skarn systems containing a near-central Lead-Zinc-Silver-Copper±Gold-Molybdenum-Tungsten), peripheral Gold-Zinc-Lead-Arsenic, and distal Lead-Zinc-Silver-Gold skarn replacements (Yilmaz, 2003). Nevertheless, proximal or distal skarn alteration and metal-bearing stockwork quartz veins/veinlets in the porphyry intrusions or serpentinites has not been recognized yet.

Table 2.1 Representative of reserve or resource values for orogenic precious/base metal mineralizations in Eskişehir-Sivrihisar region, Western Anatolia

Name	Commodity	Tectonic belt	Host rock	Deposit Type	Age of host rock	Ore body and Structure	Mineral reserve/resources	Status	Reference
Türkmen	Pb, Zn, Ag, Cu, As, Mo	Anatolid-Taurid	Granodiorite, monzodirite porphyry	Epithermal (Orogenic)	Eocene	Not known	Very significant Cu, Pb, Zn, Ag, Mo, As in soil	Prospect	Yilmaz (2003)
Mayıslar	Pb, Zn, Ag, Cu, As, Mo, Sb	Karakaya	Diorite porphyry, microdiorite	Porphyry (inrusion-related)	Eocene	Quartz veinlet	0.5 g/t Au (grab sample)	Prospect	Parlak and Sayılı (2012)
Kızılcaören	REE, Th, Ag	Anatolid-Taurid	Metasandstones, pyroclastics, trachytic porphyry, phonolites	Epithermal (volcanogenic)	Oligo-Miocene	Infilling of radial circular and funnel shaped fractures and five breccia pipes with fluorite, barite and REE	(30 Mt@3.14% REE, 37.44% CaF2,31.04% BaSO4; 0.384 Mt@0.212% ThO2 in bastnasite	Prospect	Özgenç, 1993
Okcu	Ag	Anatolid-Taurid	Marble, metaclastic, metacarbonate	Epithermal (Orogenic)	Mesozoic	Silicified carbonates, metacarbonate	Rockchip (max): 11 g/t Ag	Prospect	Eurogold, 1996
Damdamca	Au, Ag, As	Anatolid-Taurid	Marble, metaclastic, metacarbonate	Epithermal (Orogenic Listwanite)	Mesozoic	Quartz vein/veinlet, breccia and replacement in silica-carbonate altered ophiolitic rocks associated with EW-trending thrust faults and shearings	Resource indicated: 1.454 Mt@ 4.07 g/t Au, 4.98 g/t Ag; Resource indicated and inferred: 1.950 Mt@ 4.9 g/t Au, 4.49 g/t Ag	Operating Mine	Koza, 2013
Topkaya	Au, Ag, As	Anatolid-Taurid	Marble, metaclastic, metacarbonate	Epithermal (Orogenic Listwanite)		Quartz vein/veinlet, breccia and replacement in silica-carbonate altered ophiolitic rocks associated with EW-trending thrust faults and shearings	Included in the above resource	Operating Mine	Koza, 2014
Akbaştepe	Au, As, Sb, W	Upper Paleozoic metamorphic schists and marble	Sakarya continent	Mesothermal (Orogenic)	Permo-Triassic	Quartz vein/veinlet, breccia and replacement in carbonate rocks associated with EW-trending thrust faults and shearings	Resource indicated: 1.943 Mt@ 12.5 g/t Au; Resource inferred: 2.788 Mt@ 10.5 g/t Au, with 1.5 Moz contained Au	Developing Mine	Koza, 2016; AK yatırım report, 2018; https://www.akyatirim.com.tr

CHAPTER 3
SAMPLING AND CHEMICAL ANALYSIS

A total of 258 BLEG, 612 -180μm stream sediment and 65 rock chip samples were from the area were obtained from the Sivrihisar-Eskişehir region. BLEG sampling was conducted with a sampling density of ~1 sample/10 km^2 according as stream system morphology, with location selection planned to exclude sediment input from higher-order streams (Figure 3.1). The BLEG results were followed up by collecting -180μm stream sediment samples from higher-order streams at a density of 4 samples per square km. Sampling and analytical techniques as well as precision set by Eurogold according to Howarth (1983) for BLEG and -180μm stream sediment were elaborated by Yilmaz et al. (2019) and therefore, the reader is referred to the article cited hereby. Digital geology was provided by MTA (2002). Singularity mapping was carried out by using A MATLAB-based code. C-A and N-S calculations were completed in Excel and PCA using SPSS. Interpolation data for rasterizing was carried out using ArcMap10.5.

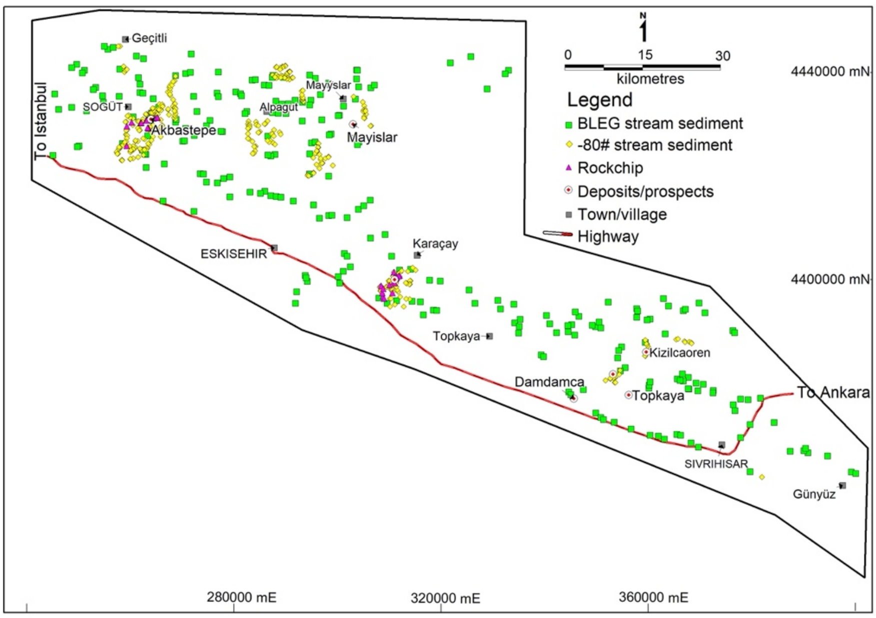

Figure 3.1 Location of important ore deposits and mineralizations along with sample points for: (a) BLEG drainage sand, (b)<180μm drainage silt, and (c) rock fragments

CHAPTER 4
MULTIFRACTAL MODELING METHODS

The C-A and N-S fractial models were used to separate populations in the geochemical data. Although such hard methods are used in the separation of geochemical populations, they are inefficient in recognizing settled and composite anomalies (Zuo & Wang, 2016). As for the soft threshold techniques, they applied spectrum-area (S-A) model and singularity mapping (SM). However, SM method has been widely used while returning robust meaningful results during statistical treatment of geochemical data (Zuo et al., 2013). On the other hand, the soft techniques are filtering methods and unearth the weak and complex geochemical signatures camouflaged by extreme values in the area under investigation (Parsa et al., 2017b). It is suggested that the soft-threshold techniques may first be used to increase the ability of anticipating the geochemical signatures and thereafter, hard-threshold techniques are used for the separation of multifractal geochemical anomalies. The singularity processes related to mineralizing events are, by definition, associated with accumulation of highly elevated metal concentrations (Helsey et al., 1993). Weak anomalies, which were not recognized because of the effects of strong background deviations or deep burial (Wang et al., 2018) can be robustly delineated. Cheng (2007) also strongly put emphasis on the concept of the singularity technique, which is useful in defining anomalies stemmed from mineral depositions and thereby forecasting the locality of unexplored ore deposits. Theory and concept of the SI (Singularity index) fractal method are described by numerous authors (Cheng et al., 2007; Helsey et al., 1993; Parsa et al., 2017a; Yilmaz et al., 2019; Zuo and Wang, 2016) and therefore, it is not necessary to repeat them in hereat.

CHAPTER 5
RESULTS

5.1 Definition of BLEG and <180µm Drainage Silt Geochem Anomalies

5.1.1 Descriptive Statistics

Histograms and Q-Q plots of BLEG Au and Ag in BLEG and gold, silver, copper, lead, zinc, arsenic and antimony in the <180µm drainage silt, along with key statistical parameters are presented in the supplement (Table 5.1 and Figures 5.1 and 5.2).

Table 5.1 Summarized statistics for BLEG Au and Ag, and minus 80# drainage silt Au, Ag, Cu, Pb, Zn, As and Sb

BLEG				
	Au ppb	**AuxCA**	**Ag_ppb**	**AgxCA**
Mean	1.4	15.2	12.72	122.1
Std. Deviation	2.9	29.2	44.64	382.5
Skewness	8.9	4.9	10.28	7.4
Kurtosis	101.9	28.4	121.81	58.8
Minimum or DL	0.0	0.3	0.01	0.1
Maximum	38.1	252.8	595.51	3763.6
N	258	258	258	258

Minus 80# stream sediment							
	Au (ppb)	**Ag (ppm)**	**Cu (ppm)**	**Pb (ppm)**	**Zn (ppm)**	**As**	**Sb**
Mean	15.2	1.2	49.7	95.2	92.5	41.2	5.4
Std. Deviation	42.9	3.5	51.6	386.1	202.3	70.3	8.7
Skewness	6.9	5.6	4.8	11.1	7.2	7.5	2.7
Kurtosis	66.8	43.7	31.7	148.1	61.0	84.7	9.1
Minimum or DL	0.3	0.0	3.0	1.0	5.0	1.0	1.0
Maximum	587.0	40.1	539.2	6292.5	2441.2	1056.6	61.7
N	612	612	612	612	612	612	612

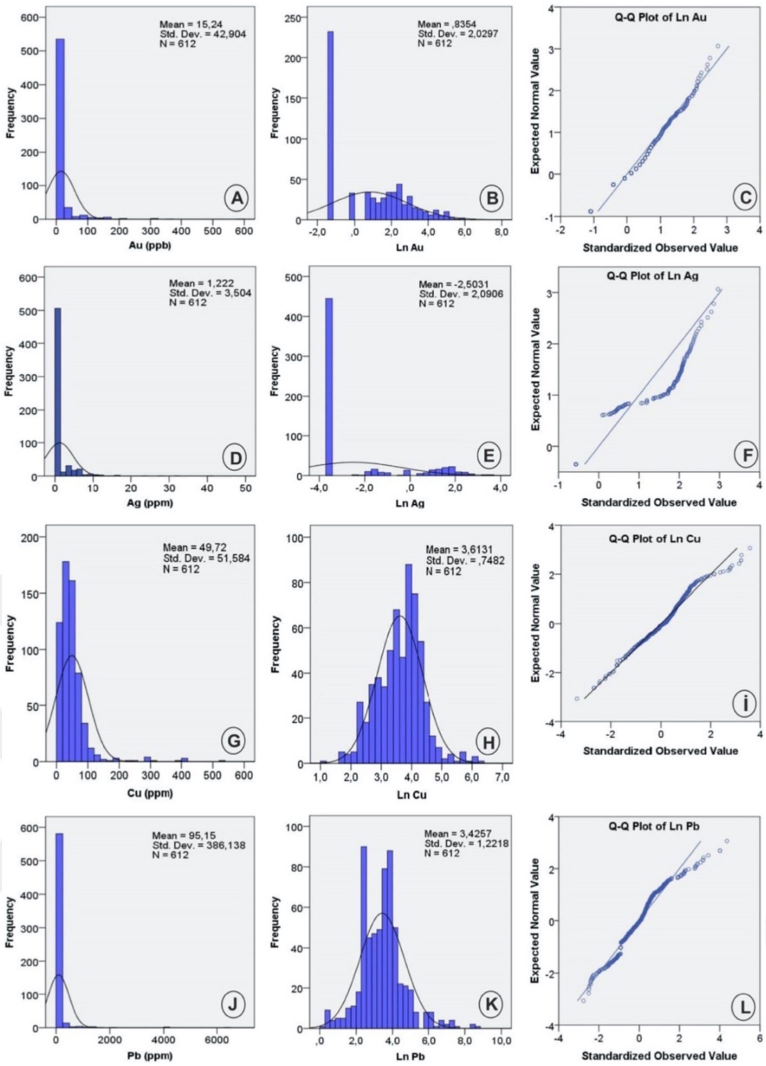

Figure 5.1 The Au, Ag, Cu, Pb, Zn, As and Sb statistical charts from the<180µm drainage silt samples in Eskişehir-Sivrihisar area

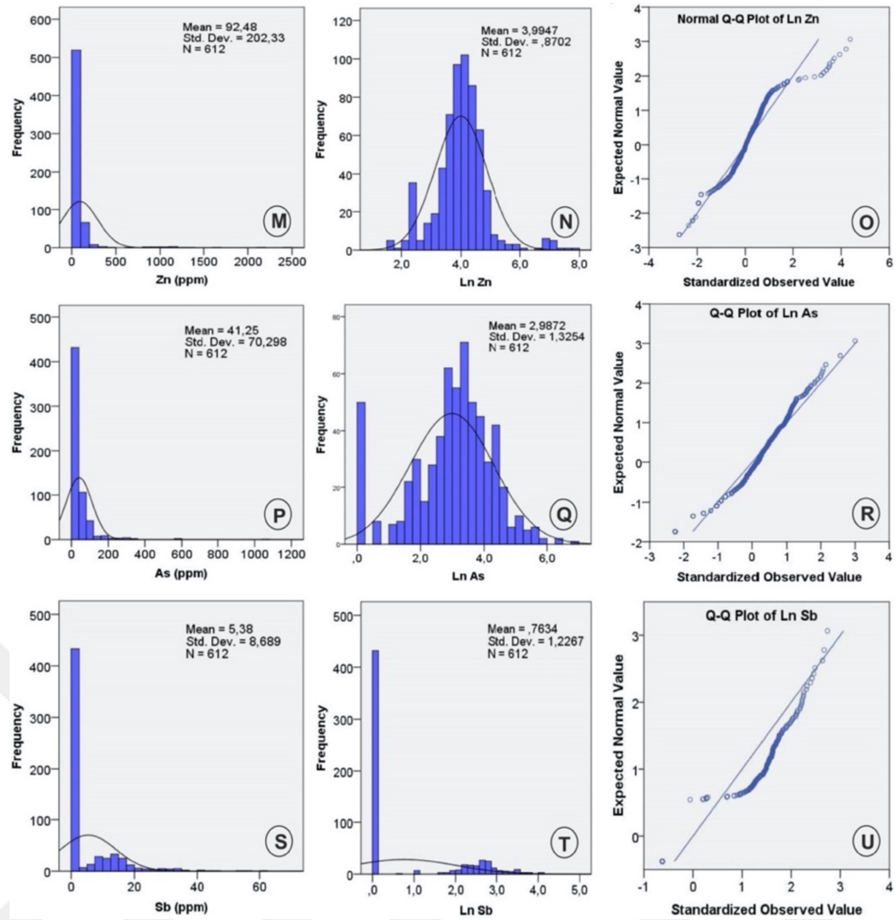

Figure 5.1 Continues

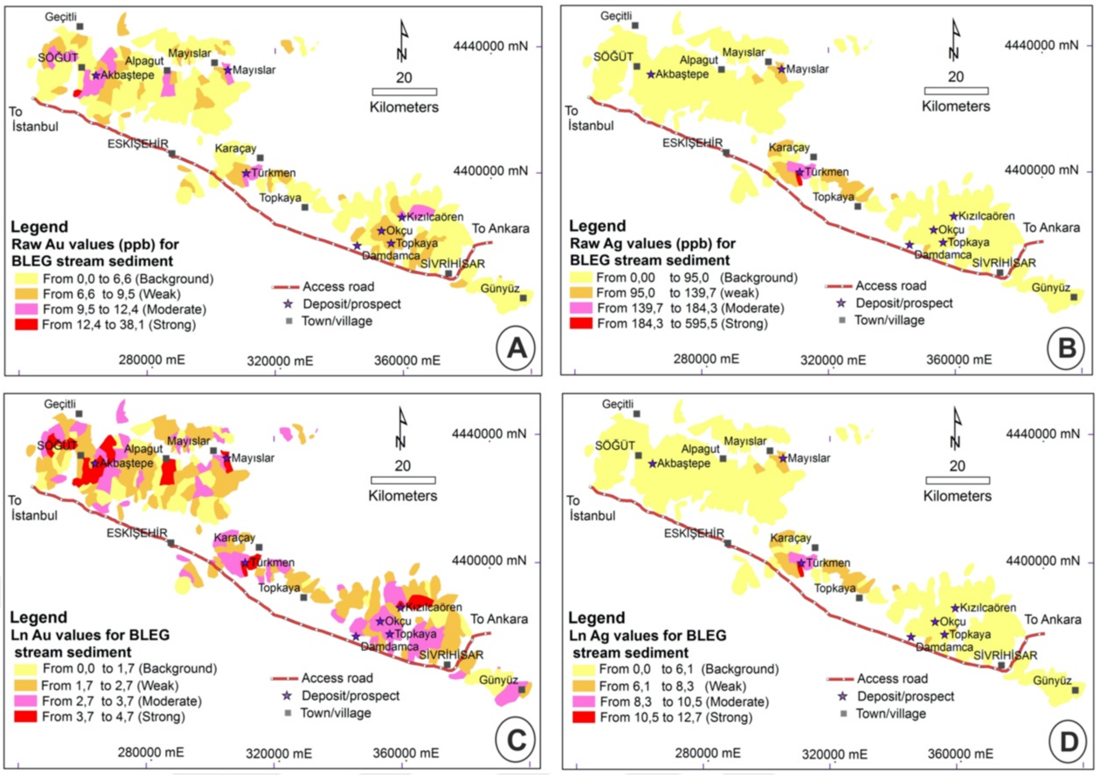

Figure 5.2 Areal extent of raw: (A) Au-anomalous and (B) Ag-anomalous areas generated bymedian+1S.D, 2SD, 3SD and 4SD, (C) Ln-tranformed Au-anomalous (D) Ln-transformed Ag-anomalous fields derived from median+1SD, 2SD, 3SD and 4SD in the Eskişehir-Sivrihisar area

5.1.2 Concentration-Area(C-A) Fractal Statistics

If the study area is treated as one mineral district without considering the effects of changing geology on geochemical background weak geochemical anomalies would not be recognized through IDW because they will be camouflaged within the background variance (Arias et al., 2012). Based on Ln-Ln design of element accumulations versus cell area with amounts higher than accumulation amounts (Figure 5.4) C-A plots for BLEG Au and AuxCA may be modeled with four (4) invariable lines compartments whereas C-A plots for BLEG Ag and AgxCA can be modeled with five (5) invariable lines sectors. For Au and AuxCA (Figure 5.4 A, B) the lines on the left-side compartment correspond to backgrounds whereas the two middle invariable segments represent low to moderate anomalies and the right-side line segments represent strong anomalies (Figure 5.4 A, B). For Ag and AgxCA (Figure 5.4 C, D) the line compartments on the left-side correspond to backgrounds whereas the three middle line segments (Figure5.4 C, D) represent low to strong anomalies and the right-hand line segments represent very strong anomalies. Figure

5.3 shows spatial distribution of BLEG Au, AuxCA, Ag, and AgxCA background, weak, moderate, strong, and very strong anomalies defined by C-A fractal modeling (Figure 5.3) and their relationship to already known deposits/prospects. As is shown in Figure 5.4, moderate Au and AuxCA anomalies encompass whole deposits/prospects (Figure 5.4 C, D) whereas strong and very strong Ag and AgxCA anomalies (Figure 5.4 C, D) cover 85% of the deposits/prospects.

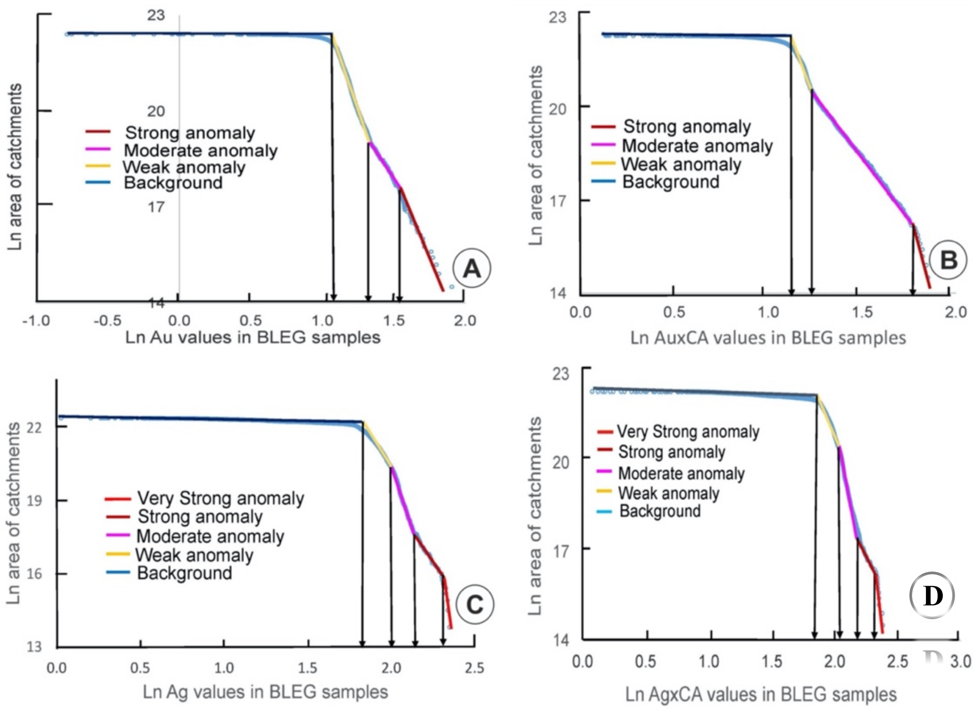

Figure 5.3 Ln-transformed C-A fractal model of (A) Au, (B) AuxCA, (C) Ag, and (D) AgxCA in BLEG samples

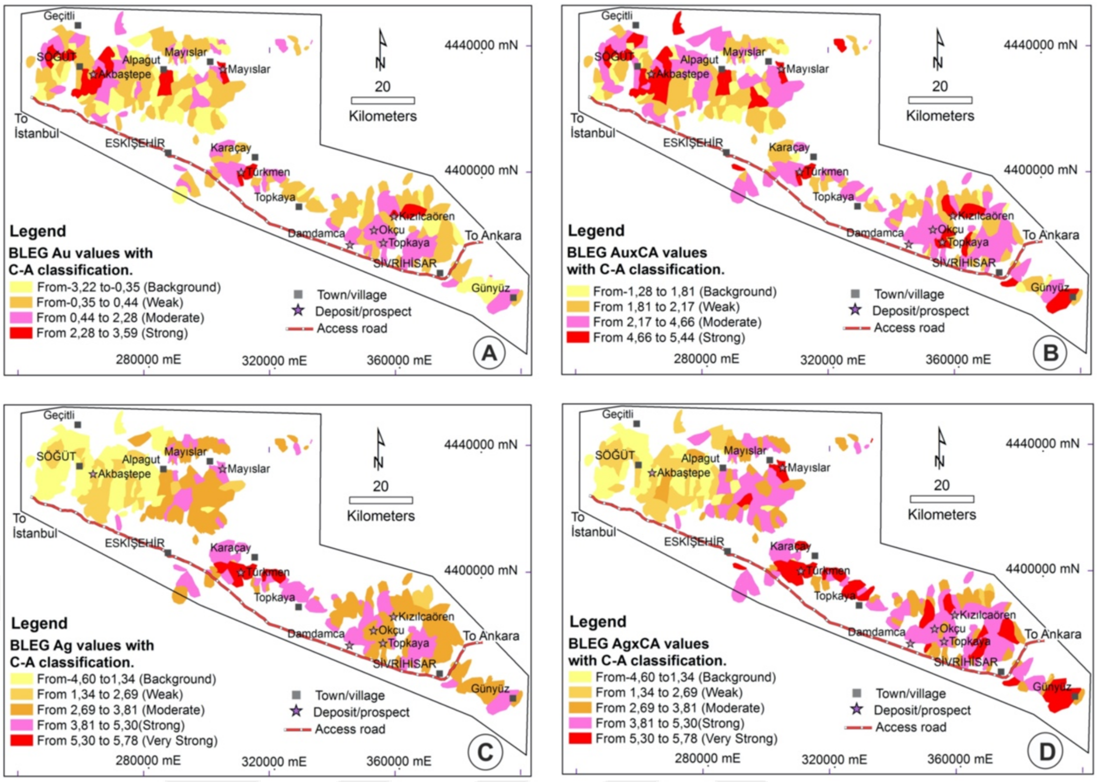

Figure 5.4 Geochemical maps of Ln-transformed BLEG: (A) Au, (B) AuxCA, (C) Ag and (D) AgxCA returned from C-A multifractal modeling

5.1.3 Spatial Patterns of Multi-element Geochemical Signatures Using C-A Statistics Model

In this study in order to extract enhanced multi-element geochemical signatures, ordinary PC as a multivariate analysis tool was applied to log-transformed data of 7 elements including gold, silver, arsenic, antimony, copper, lead, and zinc from <180µm stream sediments. Geochemical associations related to different deposit types and geochemical processes in stream systems may be obtained using PC, some of which may be interpreted as pathfinders for the deposit type including gold, silver, arsenic, antimony, copper, lead, and zinc from <180µm stream sediments. Geochemical associations related to different deposit types and geochemical processes in stream systems may be obtained using PC, some of which may be interpreted as pathfinders for the deposit type sought. As illustrated in Table 2, three components were extracted based on the significant eigenvalues (> 0.9). The PCA results demonstrated that the log-transformed <180µm stream sediments data were classified into the following two components in which the most significant elements are blackhighlighted based on the loading values of ≥ 0.5: (1) gold-copper-lead-zinc-arsenic and (2) silver-antimony. PC1 and PC2 account for ~30% and ~28% of total variability, respectively. Gold, Cu, Pb, Zn, and As have significant positive PCA1 loadings and represent the effects of porphyry and skarn-related mineralization- in the study area. PC2 is representative of Ag and Sb mineralization. C-A and N-S fractal models were implemented to PCA scores (Figure 5.5) for comparison with the BLEG and BLEG Au-AgxCA and BLEGxCA Au-Ag models. The C-A fractal model indicated four BLEG Au-Ag or BLEGxCA Au-Ag populations (Figure 5.6). The N-S fractal model of PC1 returned 5 distinct geochemical populations of strong, moderate, and weak anomalies plus backgrounds for Au in <180µm values (Figure 5.6 E, F) whereas PC2 of the <180µm stream sediment data was classified into 3 populations. Gold mineralization of the area is mainly confined to the moderate to strong anomaly zones of PC1 BLEG values whereas the Akbaştepe deposit is located in the background zone of PC1 of BLEGxCA data with others occurring mostly in moderately anomalous zones (Figure 5.6 B, D). The efficiency of PCA method is evaluated using five mineral deposits/prospects. Four of these mineralizations of the investigated region fall over moderate to strong anomaly zones of PC1 with positive Au-Cu-Pb-Zn-As loadings ≥ 0.5 (80% efficiency) whereas PC2 has 40% efficiency (Figure 5.6 E-H).

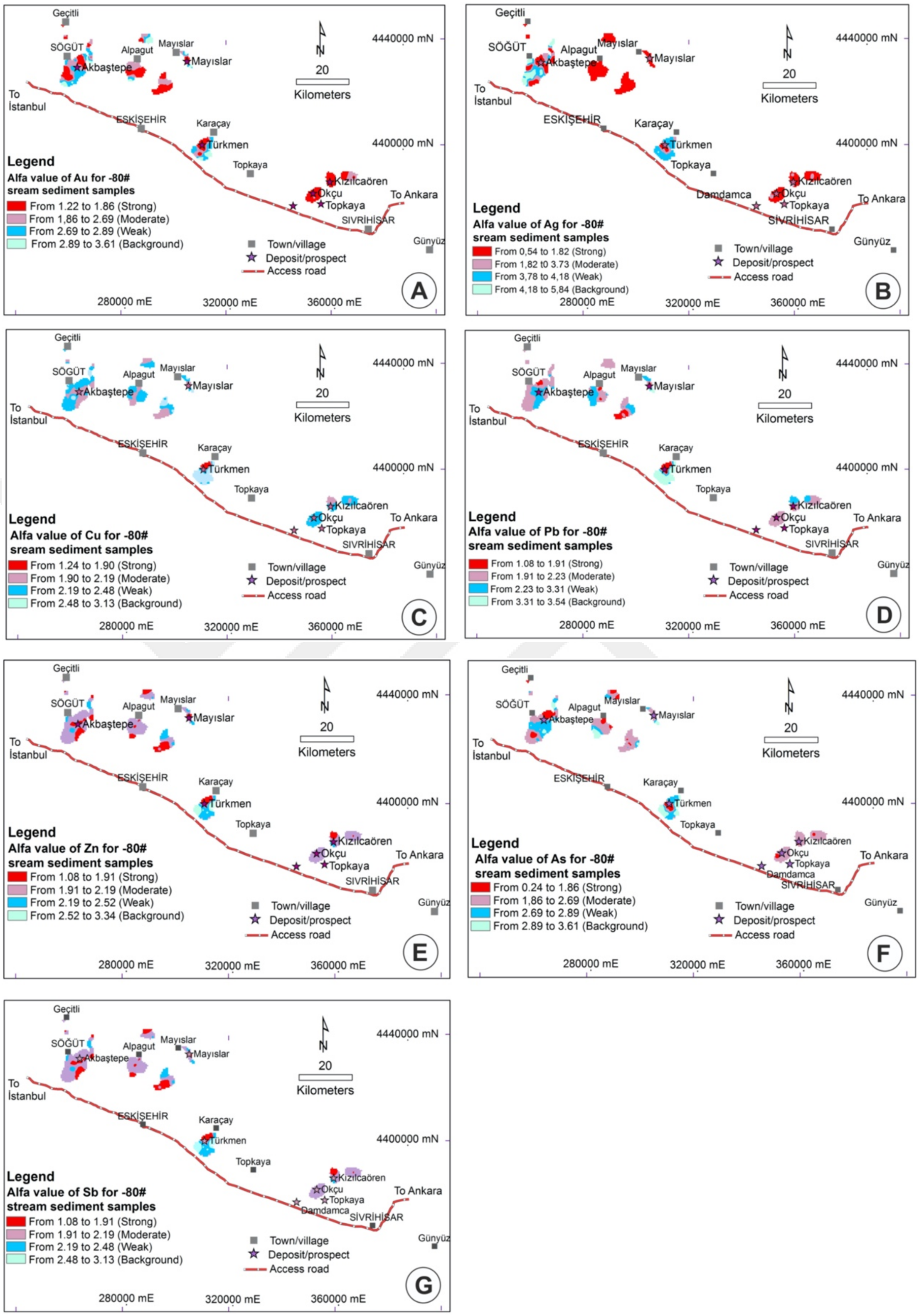

Figure 5.5 Raster map exhibiting alfa-values of the drainage silt: (A) Au, (B) Ag, (C) Cu, (D) Pb, (E) Zn, (F) As and (G) Sb accumulations predicted using the window-based method

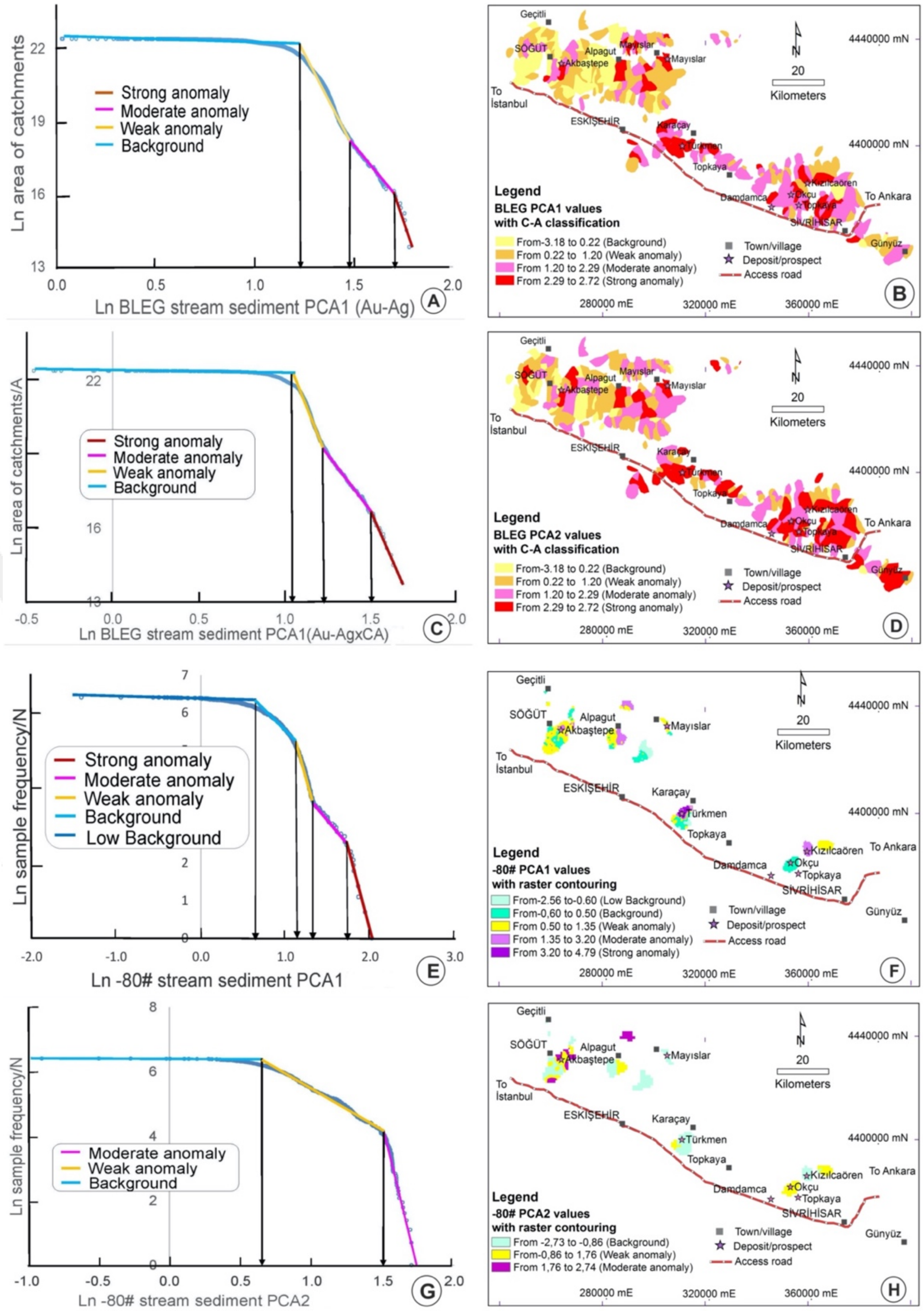

Figure 5.6 PCA1 with fractal models and delineated geochemical anomaly population maps of (A, B), Au, (C, D) AuxCA in BLEG samples; PCA1 and PCA2 with fractal models and delineated geochemical anomaly population maps of loaded Au+Cu+Pb+Zn+As (E, F) and Ag+Sb (G,H) in <180μm stream sediment samples

5.1.4 Spatial Patterns of Mono-element Geochemical Signatures Using C-A and N-S Statistics Model in BLEG and <180µm Stream Sediment Data

To augment the geochemical characteristics, the singularity mapping has been implemented to the geochemical results of BLEG and <180µm stream sediment samples. Gold and AuxCA α values ranged from 1.13 to 2.66 and 1.17 to 3.26, respectively whereas for Ag and AgxCA ranged from 1.17 to 3.27 and 0.95 to 3.62, respectively. The C-A fractal model of singularity indexes (Figure 5.7) indicated four distinct Au geochemical populations for BLEG Au data (Figure 5.7 A). In the same way, the C-A fractal model has identified 5 geochemical groups ranging from strong through moderate to weak anomalies as well as background and low backgrounds for AuxCA, Ag, and AgxCA (Figure 5.7 B, C, D). Figure 5.7 E, F, G, H also illustrates the areal dispersal of identified geochemical groups. Gold mineralizations that are explored in the study area are confined to the strong and moderate Au and AuxCA BLEG anomaly zones (Figure 5.7 E, F). Singularity anomaly patterns coincide much on pointing to mineralization and carbonate-mica altered metamorphic rocks in the western part (Akbaştepe/Söğüt), argillic-chlorite-talc-altered ophilites in the central part (Türkmen), and argillic-altered high-pressure metamorphic rocks in the eastern part (Topkaya, Damdamca, Okçu, Kızılören) of the study area.

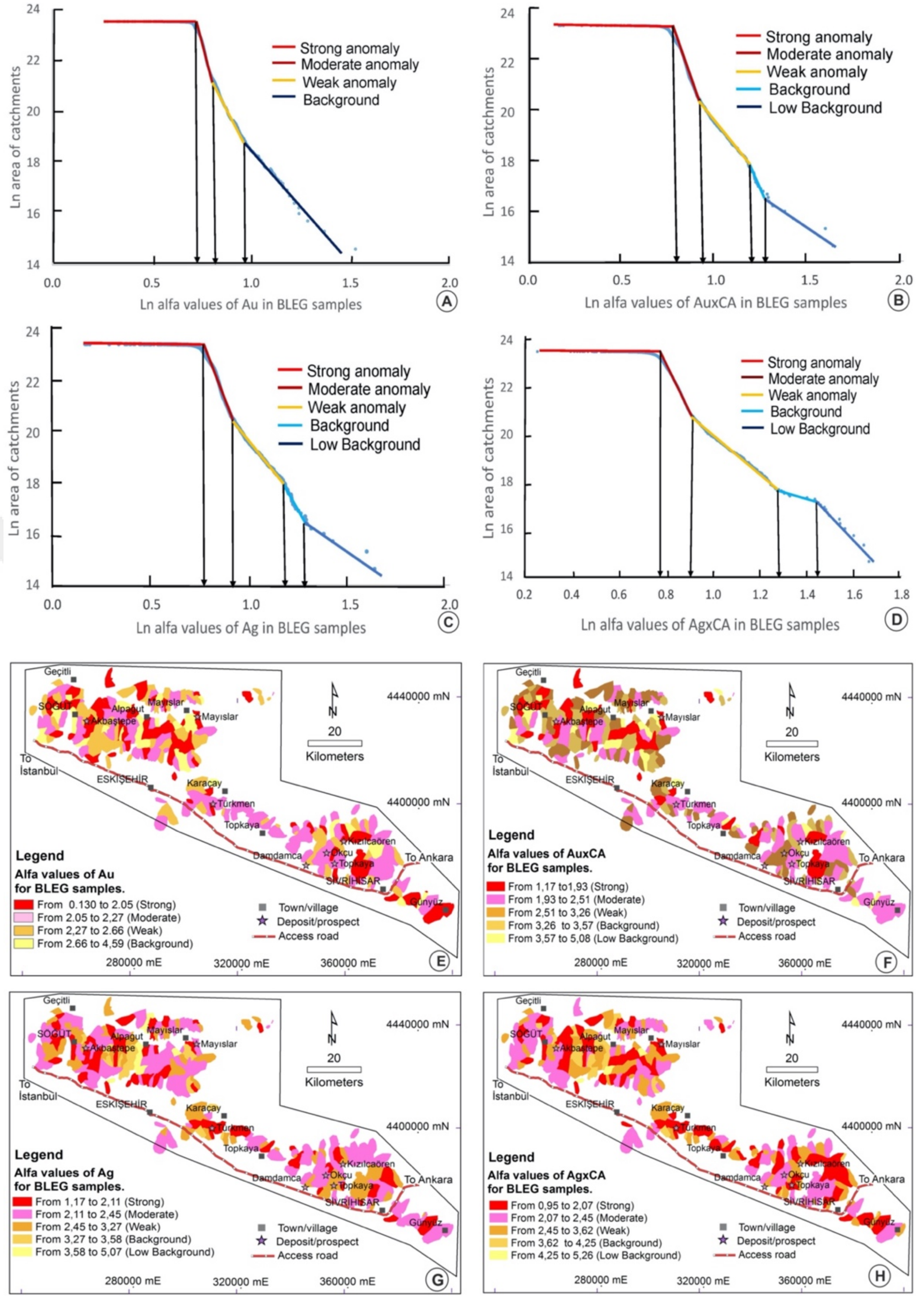

Figure 5.7 Concentration-Area fractal model applied to singularity indexes of: (A) Au, (B) AuxCA, (C) Ag and (D) AgxCA and delineated geochemical anomaly population of (E) Au, (F) AuxCA, (G) Ag and (H) AgxCA in BLEG samples

5.1.5 Delineation of <180µm Drainage Silt Geochem Anomalies

-180 µm drainage silt samples were assayed for gold, copper, lead, zinc, arsenic, and antimony. The statistical study of above-mentioned elements has shown that they were positively skewed dispersal (Table 5.1) and in this way they likely contain multiple populations. Therefore, multifractal analysis was implemented to delineate geochemical populations of these elements. The results of geochemical analyses of -80# stream sediments were initially subjected to singularity multifractal technique. To model the areal dispersion of the SI α values, a square window-based singularity mapping method was applied as individual samples cannot be directly linked to unique catchment basins. Four different classes of geochem signatures of gold, arsenic, antimony were obtained using N-S fractal model (Figure 5.8 A, F, G) whereas the 5 geochemical populations were received for the geochemical signature of silver, copper, lead, and zinc in drainage silt data (Figure 5.8 B, C, D, E). The geographical dispersion maps of <180µm drainage silt α-gold, α-copper, α-silver, α-lead, α-zinc, α-arsenic, and α-antimony show low singularity anomaly values (Figure 5.5). Akbaştepe, Mayıslar, Türkmen, Okçu and Kızılcaören deposits fall over the areas with low α-gold, α-silver, α-zinc singularity values whereas Türkmen base metal deposit is defined by high α-gold, α-copper, α-silver, α-lead, α-zinc, α-arsenic and α-antimony singularity values. To quantitatively measure the geographical correlation between areas with α and the locality of known Au deposits, the singularity maps of gold, silver, copper, lead, zinc, arsenic and antimony (Figure 5.5 A, G), and the α values were re-categorized implementing the Number-Size fractal model. The already-discovered gold mineralizations are nearly related to the lower α values (generally less<2.2) of gold, silver, copper, lead, zinc, arsenic, and antimony (Figure 5.5) despite the slightly differ in the geographic distribution of gold, copper, lead, zinc, arsenic and antimony anomalies. Besides, 100% (5), 100% (5), 60% (3), 80% (4), 100% (5), 100% (5), 60% (3) of known deposits coincide with the moderate to strong anomalies of gold, copper, lead, zinc, arsenic and antimony anomalies, respectively (Figure 5.9). This suggests that gold, silver, lead, zinc, and arsenic are suitable pathfinder elements in the Eskişehir district as the singularity mapping technique may recognize precious/base metal deposits/prospects.

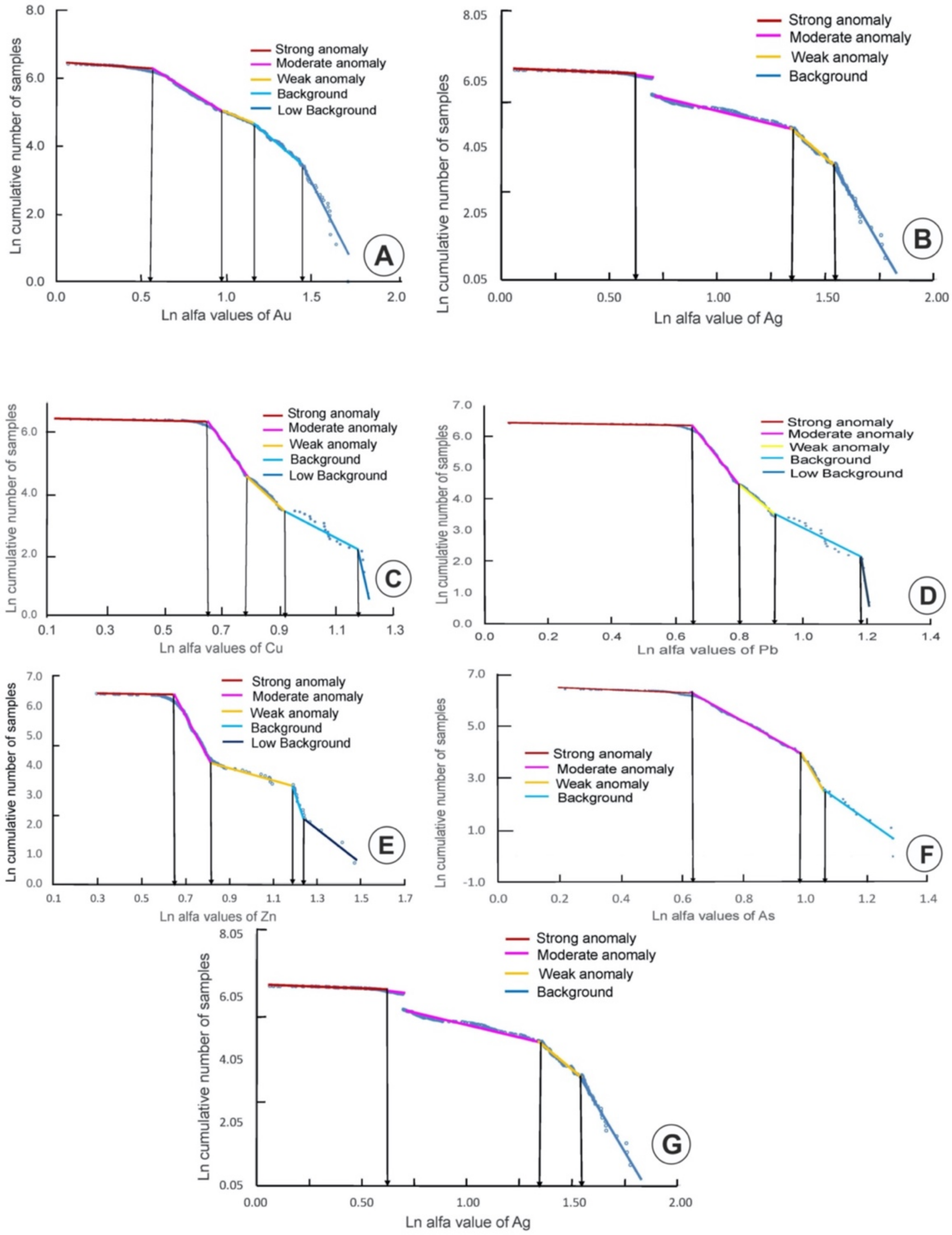

Figure 5.8 Applied Number-Size fractal model to singularity indexes of: (A) Gold, (B) Silver, (C) Cu, (D) Pb, (E) Zn, (F) As and (G) Sb in <180µm stream sediment samples

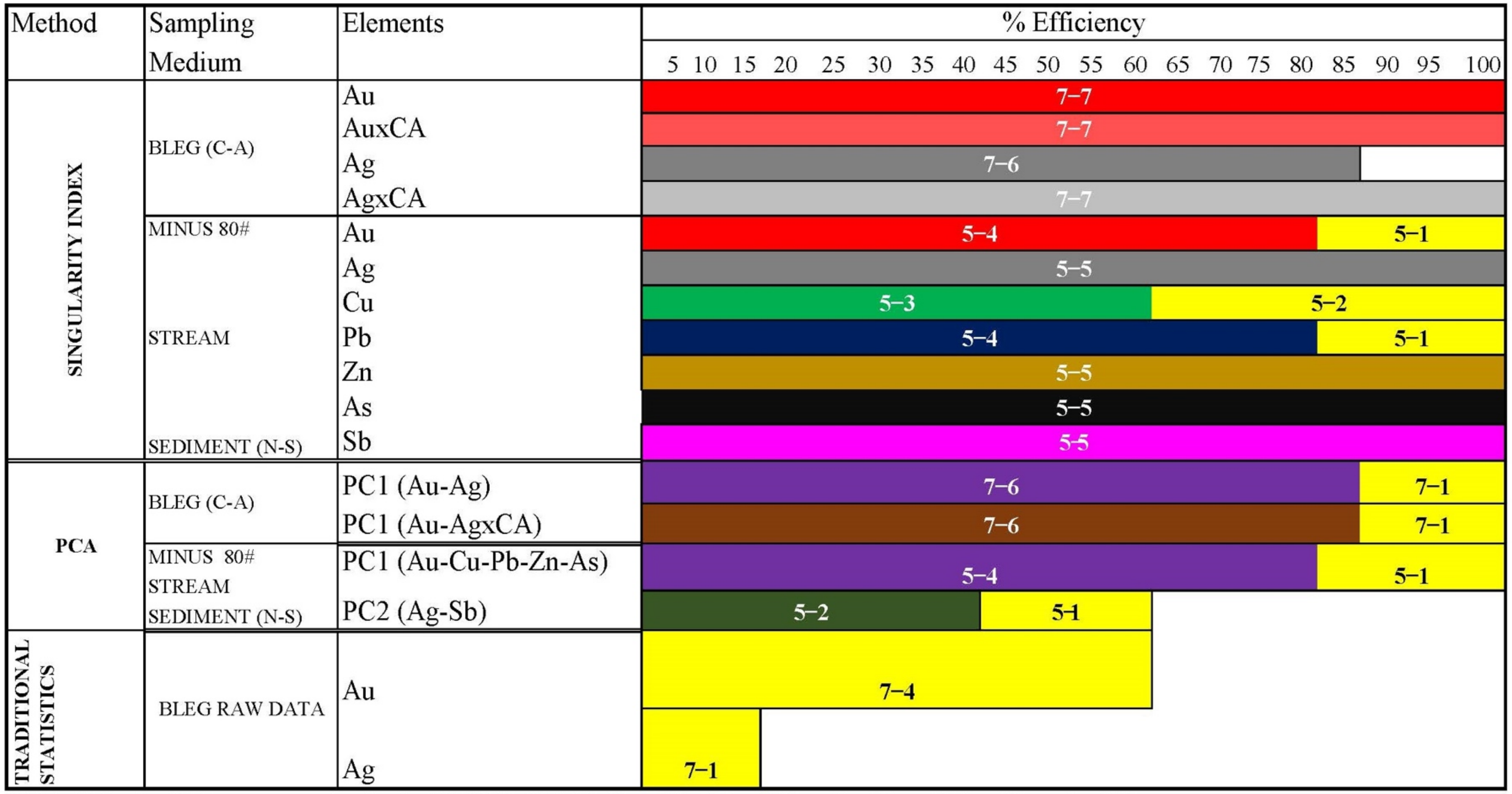

PCA: Principal Component Analysis, TP/(TP+FN)%: True Positive/(True Positive+False Negative)%

Yellow color shows weak anomaly, white color indicetes background and other colors refer to moderate to strong anomalies.

Figure 5.9 BLEG and −80# stream sediment sample population classifications (number of known deposits/prospects in falling in areas of populations with different strengths) using several fractal and traditional statistical plots for Au, Ag and other elements

5.1.6 Verification of The Anomalies Delineated

Figure 5.9 shows the effectiveness of assessment of the delineated BLEG and <180µm stream sediment geochemical anomalies regarding the already-discovered gold mineralizations of the Eskişehir district. In accordance with Figures 3-8, >85% of known gold and base metal deposits are located within the Au, AuxCA, Ag and AgxCA based on the singularity index, C-A fractal analysis and PCA. However, these values are highly variable for -80 stream sediment data. 100% of already-discovered deposits are located within the anomaly areas of <180µm stream sediment Zn, As and Sb based on singularity and log-transformed data with N-S fractal modeling (Figure 5.9). Besides, singularity index and log-transformed data of <180µm Ag and Cu with N-S fractal modeling also returned moderate to strong anomalies encompassing 100% of the deposits and prospects. Judgement of rock-chip sample results proves the power of the BLEG and <180µm drainage silt sampling in accurate recognition of orogenic gold-arsenic-antimony-tungsten (Akbaştepe), copper-lead-zinc-arsenic-molybdenum (Mayıslar), copper-lead-zinc—silver-arsenic-antimony-gold (Türkmen) and gold-silver deposits (west of Sivrihisar Town). The anomalous zones (strong-moderate anomaly) of BLEG Au suggest that these areas deserve additional exploration campaigns. The BLEG and <180µm stream sediment geochemical Au and Ag, as well as base metal anomalies recognized, are encompassed by illite-sericite-silica-bearing rocks, and therefore, are of high-priority targets for supplementary exploration in addition to the already discovered occurrences (Figure 5.3-Figure 5.5).

CHAPTER 6
DISCUSSION AND CONCLUSIONS

The strength of stream sediments geochemical anomalies typically diminishes downstream due to dilution of element abundances (Parsa et al., 2017b; Yilmaz et al., 2019), in addition to errors induced by sampling and analytical errors (Parsa et al., 2016a, c) coupled with smoothing effect by moving average interpolation methods (Yousefi, 2017; Yuan et al., 2015). Nevertheless, multifractal interpolation techniques may use singularity and moving average interpolation to concurrently calculate local singularities and the spatial correlation among values, thereby also defeating the flattening consequence of applying a moving average interpolation method (Cheng, 1999). These techniques clarify the diagnosis of geochemical groups by amplifying geochemical anomalies and segregating from geochemical background values (Cheng, 2000; Yuan et al., 2015). Hard threshold techniques are not always able to identify weak anomalies (e.g., C-A fractal modeling), particularly in intensely altered lateritic covers (Shuguang et al., 2015). However, when singularity mapping (Cheng, 1999; 2007) are implemented as soft threshold techniques, numerous discoveries of weak geochemical anomalies have been encountered quite often (Yousefi, 2017a, b; Yuan et al., 2015; Zuo et al., 2015). Once the localized singularity indexes (*alfa*- values) are amalgamated in multifractal moving average interpolation, as in this investigation, the MIDW-interpolated geochemical values correspond to amplified geochemical models, permitting for the identification of fainted anomalies (Parsa et al. 2017). BLEG stream sediment Au and Ag anomalies highly correlate with those of <180 µm stream sediment abnormalities. Besides, gold-rich rock-chip assays as well as the discovery of mineralizations in the recognized zones of BLEG and <180µm stream sediment anomalies suggested that these BLEG and <180µm stream sediment anomaly zones without undetected mineralizations deserve further exploration. BLEG Au and Ag geochemical signatures derived from SI, C-A, N-S and PCA multifractal techniques can justify gold deposition in the area of investigation due to the affiliation of BLEG geochemical signatures with Au deposition (Figure 5.3-5.9). Besides, <180µm stream sediments singularity index Au and Ag geochemical anomalies have strong geographic alliance with Au precipitation within the areas of argillic and silicic alterations. Moreover, the singularity index-based geochemical signatures of the lead-zinc-arsenic-antimony and C-A fractal values of copper-lead-zinc-arsenic elements in <180μm drainage silt samples show strong association to gold mineralization (Figure 5.10). Even, <180μm stream sediments with PCA1 loadings ≥ 0.5 (Au-Cu-Pb-Zn-As) display strong association with known ore deposits at an 80% efficiency level. Au and Ag geochemical anomalies derived from raw BLEG data have an association with known deposits with 85% and 15% underlain by moderate to weak anomalies and background, respectively (Figure 5.2 and Figure 5.9) whereas Log-transformed BLEG Au and Ag signatures display association with the known deposits at 100% and 30 efficiency level, respectively. It seems that IDW interpolation of Log-transformed Au anomalies derived from median +2σ, 3σ and 4σ detected all the deposits/prospects. However, multifractal analysis also generates additional moderate to strong, even weak, BLEG Au and Ag anomalies, which are targets for discovering significant Au deposits (Figure 5.3 C, D and Figure 5.4-Figure 5.7). This shows that multifractal analysis is robust and very efficient in identifying ore-related geochemical anomalies. The geochemical anomalies derived from SI, C-A, N-S and PCA fractal/multifractal techniques should be combined with further prospecting and structural mapping as well as MMI soil sampling. This would probably give way to the identification of new mineralization sites study area underlain by low α values <2. Also shown that the common square window-based singularity mapping method appears to be an effective tool in identifying geochemical abnormalities with ore potential.

REFERENCES

Afzal, P., Alghalandis, Y. F., Khakzad, A., Moarefvand, P., & Omran, N. R. (2011). Delineation of mineralization zones in porphyry Cu deposits by fractal concentration–volume modeling. *Journal of Geochemical exploration*, *108*(3), 220-232.

Afzal, P., Khakzad, A., Moarefvand, P., Omran, N. R., Esfandiari, B., & Alghalandis, Y. F. (2010). Geochemical anomaly separation by multifractal modeling in Kahang (Gor Gor) porphyry system, Central Iran. *Journal of Geochemical Exploration*, *104*(1-2), 34-46.

Agterberg, F. P., Bonham-Carter, G. F., & Wright, D. F. (1990). Statistical pattern integration for mineral exploration. In *Computer applications in resource estimation* 1-21.

Altıner, D., Koçyiğit, A., Farinacci, A., Nicosia, U., & Conti, M. A. (1991). Jurassic, Lower Cretaceous stratigraphy and paleogeographic evolution of the southern part of north-western Anatolia. *Geologica Romana*, *28*, 13-80.

Arias, M., Gumiel, P., & Martín-Izard, A. (2012). Multifractal analysis of geochemical anomalies: A tool for assessing prospectivity at the SE border of the Ossa Morena Zone, Variscan Massif (Spain). *Journal of Geochemical Exploration*, *122*, 101-112.

Bonham-Carter, G. F., & Goodfellow, W. D. (1986). Background corrections to stream geochemical data using digitized drainage and geological maps: application to Selwyn Basin, Yukon and Northwest Territories. *Journal of Geochemical Exploration*, *25*(1-2), 139-155.

Bonham-Carter, G. F., Rogers, P. J., & Ellwood, D. J. (1987). Catchment basin analysis applied to surficial geochemical data, Cobequid Highlands, Nova Scotia. *Journal of Geochemical Exploration*, *29*(1-3), 259-278.

Carranza, E. J. M. (2010a). Catchment basin modelling of stream sediment anomalies revisited: incorporation of EDA and fractal analysis. *Geochemistry: Exploration, Environment, Analysis*, *10*(4), 365-381.

Carranza, E. J. M. (2010b). Mapping of anomalies in continuous and discrete fields of stream sediment geochemical landscapes. *Geochemistry: Exploration, Environment, Analysis*, *10*(2), 171-187.

Chen, X., Zheng, Y., Xu, R., Wang, H., Jiang, X., Yan, H., ... & Guo, X. (2016). Application of classical statistics and multifractals to delineate Au mineralization-related geochemical anomalies from stream sediment data: a case study in Xinghai-Zeku, Qinghai, China. *Geochemistry: Exploration, Environment, Analysis*, *16*(3-4), 253-264.

Cheng, Q. (2007). Mapping singularities with stream sediment geochemical data for prediction of undiscovered mineral deposits in Gejiu, Yunnan Province, China. *Ore Geology Reviews*, *32*(1-2), 314-324.

Cheng, Q., Agterberg, F. P., & Ballantyne, S. B. (1994). The separation of geochemical anomalies from background by fractal methods. *Journal of Geochemical exploration*, *51*(2), 109-130.

Cheng, Q., Agterberg, F. P., & Bonham-Carter, G. F. (1996). A spatial analysis method for geochemical anomaly separation. *Journal of Geochemical exploration*, *56*(3), 183-195.

Cheng, Q., Xu, Y., & Grunsky, E. (2000). Integrated spatial and spectrum method for geochemical anomaly separation. *Natural Resources Research*, *9*(1), 43-52.

Chiprés, J. A., Castro-Larragoitia, J., & Monroy, M. G. (2009). Exploratory and spatial data analysis (EDA–SDA) for determining regional background levels and anomalies of potentially toxic elements in soils from Catorce–Matehuala, Mexico. *Applied Geochemistry*, *24*(8), 1579-1589.

Deng, J., Wang, Q., Yang, L., Wang, Y., Gong, Q., & Liu, H. (2010). Delineation and explanation of geochemical anomalies using fractal models in the Heqing area, Yunnan Province, China. *Journal of Geochemical Exploration*, *105*(3), 95-105.

Eurogold, 1996. Review report on gold anomalies and prospects generated between 1991 and 1996 in western Turkey. *Unpublished Company Report*.

Fletcher, K., & Horsky, S. (1988). Determination of gold by cyanidation and graphite furnace atomic absorption spectroscopy. *Journal of Geochemical Exploration*, *30*(1-3), 29-34.

Fletcher, W. K., & Gubins, A. G. (1997). Stream sediment geochemistry in today's exploration world. In *Proceedings of Exploration* (97, 249-260). Retrieved October 27, 2021, from https://www.911metallurgist.com/blog/wp-content/uploads/2015/10/Stream-Sediment-Geochemistry-in-Todays-Exploration-World.pdf.

Ghezelbash, R., Maghsoudi, A., Daviran, M., & Yilmaz, H. (2019). Incorporation of principal component analysis, geostatistical interpolation approaches and frequency-space-based models for portraying the Cu-Au geochemical prospects in the Feizabad district, NW Iran. *Geochemistry*, *79*(2), 323-336.

Govett, G. J. S., Goodfellow, W. D., Chapman, R. P., & Chork, C. Y. (1975). Exploration geochemistry—distribution of elements and recognition of anomalies. *Journal of the International Association for Mathematical Geology*, *7*(5), 415-446.

Grunsky, E. C. (2010). The interpretation of geochemical survey data. *Geochemistry: Exploration, Environment, Analysis*, *10*(1), 27-74.

Grunsky, E. C. (2007). The interpretation of regional geochemical survey data. In *Proceedings of Exploration, 7*, 384-404.

Hawkes, H. E. (1976). The downstream dilution of stream sediment anomalies. *Journal of Geochemical Exploration*, *6*(1-2), 345-358.

He, J. Z., Yao, S. Z., Zhang, Z. P., & You, G. J. (2013). Complexity and productivity differentiation models of metallogenic indicator elements in rocks and supergene media around Daijiazhuang Pb–Zn deposit in Dangchang County, Gansu Province. *Natural Resources Research*, *22*(1), 19-36.

Helsey TC., Jensen MH., Kadanoff LP., Procaccia I., & Shraiman BI. (1993). *Fractal measures and their singularities: the characterization of strange sets*. In 'From Order to Chaos: Essays: Critical, Chaotic and Otherwise, 443-453. Retrieved October 27, 2021, from https://www.sciencedirect.com/science/article/abs/pii/0920563287900363.

Koza Gold, (2013). *Koza Gold Company report (unpublished).*

Lin, X., Zhang, B., & Wang, X. (2014). Application of factor analysis and concentration-volume fractal modeling to delineation of 3D geochemical patterns: a case study of the Jinwozi gold field, NW China. *Geochemistry: Exploration, Environment, Analysis*, *14*(4), 359-367.

Luz, F., Mateus, A., Matos, J. X., & Gonçalves, M. A. (2014). Cu-and Zn-soil anomalies in the NE border of the south Portuguese zone (Iberian Variscides, Portugal) identified by multifractal and geostatistical analyses. *Natural Resources Research*, *23*(2), 195-215.

Mandelbrot, B. B.(1983). *The fractal geometry of nature* (Vol. 1). New York: WH freeman.

Meier, A. L. (1980). Flameless atomic-absorption determination of gold in geological materials. *Journal of Geochemical Exploration*, *13*(1), 77-85.

MTA (Maden Tetkik ve Arama Enstitüsü), (1965). *Tungsten and Molybdenum Deposits of Turkey.* Ankara: MTA Yayınları. 128, Ankara. Retrieved October 27, 2021, from https://www.bestfilebook.com/pdf/tungsten-and-molybdenum-deposits-of-turkey/.

MTA (Maden Tetkik ve Arama Enstitüsü), (1970). *Arsenic, Mercury, Antimony and Gold Deposits. MTA, 2002. 1:500000 Geological map of Turkey*. MTA (Geological Survey Turkey), Ankara. Retrieved October 27, 2021, from https://ebooksumo.com/search/arsenic-mercury-antimony-and-gold-deposits-of-turkey/.

Okay, A. I., & Satir, M. (2000). Coeval plutonism and metamorphism in a latest Oligocene metamorphic core complex in northwest Turkey. *Geological Magazine*, *137*(5), 495-516.

Okay Aİ., Satır M., Maluski H., Siyako M., Monie P., Metzger R., & Akyüz S. (1996). Paleo- and Neo- Tethyan events in northwest Turkey: geological and geochronological constraints*. In: Yin, A. and Harrison, M. (Eds), Tectonics of Asia.* 420–441. Cambridge University Press.

Okay, A., & Satir, M. (2006). Geochronology of Eocene plutonism and metamorphism in northwest. *Geodinamica Acta*, *19*(5), 251-266.

Özgenç, İ. (1993). Geology and REE-geochemistry of carbothermal bastnaesite–fluorite–barite deposit of Kızılcaören (Sivrihisar, Eskişehir). *Geological Bulletin of Turkey*, *36*, 1-11.

Parlak, B., & Sayili, I. S. (2012). Fluid inclusion data on quartz and calcite in alteration zones of polymetallic mineralizations at Mayislar area (Saricakaya-Eskisehir, Turkey). *Türkiye Jeoloji Bülteni-Geological Bulletin of Turkey, 55*(2), 111-136.

Parsa, M., Maghsoudi, A., & Ghezelbash, R. (2016). Decomposition of anomaly patterns of multi-element geochemical signatures in Ahar area, NW Iran: a comparison of U-spatial statistics and fractal models. *Arabian journal of Geosciences*, *9*(4), 260.

Parsa, M., Maghsoudi, A., Yousefi, M., & Sadeghi, M. (2017a). Multifractal analysis of stream sediment geochemical data: Implications for hydrothermal nickel prospection in an arid terrain, eastern Iran. *Journal of Geochemical Exploration*, *181*, 305-317.

Parsa, M., Maghsoudi, A., Yousefi, M., & Carranza, E. J. M. (2017b). Multifractal interpolation and spectrum–area fractal modeling of stream sediment geochemical data: Implications for mapping exploration targets. *Journal of African Earth Sciences*, *128*, 5-15.

Reimann, C., & Filzmoser, P. (2000). Normal and lognormal data distribution in geochemistry: death of a myth. Consequences for the statistical treatment of geochemical and environmental data. *Environmental geology*, *39*(9), 1001-1014.

Reimann, C., Filzmoser, P., & Garrett, R. G. (2002). Factor analysis applied to regional geochemical data: problems and possibilities. *Applied geochemistry*, *17*(3), 185-206.

Reimann, C., Filzmoser, P., & Garrett, R. G. (2005). Background and threshold: critical comparison of methods of determination. *Science of the total environment*, *346*(1-3), 1-16.

Ren, L., Cohen, D. R., Rutherford, N. F., Zissimos, A. M., & Morisseau, E. G. (2015). Reflections of the geological characteristics of Cyprus in soil rare earth element patterns. *Applied Geochemistry*, *56*, 80-93.

Rose AW., Hawks HE., Webb JH. (1979). *Geochemistry in Mineral Exploration*. NewYork: Academic Press.

Sadeghi, B., Madani, N., & Carranza, E. J. M. (2015). Combination of geostatistical simulation and fractal modeling for mineral resource classification. *Journal of Geochemical Exploration*, *149*, 59-73.

Shen, W., & Cohen, D. R. (2005). Fractally invariant distributions and an application in geochemical exploration. *Mathematical Geology*, *37*(8), 895-913.

Shuguang, Z., Kefa, Z., Yao, C., Jinlin, W., & Jianli, D. (2015). Exploratory data analysis and singularity mapping in geochemical anomaly identification in Karamay, Xinjiang, China. *Journal of Geochemical Exploration*, *154*, 171-179.

Sinclair, A. J. (1991). A fundamental approach to threshold estimation in exploration geochemistry: probability plots revisited. *Journal of Geochemical Exploration*, *41*(1-2), 1-22.

Spadoni, M. (2006). Geochemical mapping using a geomorphologic approach based on catchments. *Journal of Geochemical Exploration*, *90*(3), 183-196.

Spadoni, M., Voltaggio, M., & Cavarretta, G. (2005). Recognition of areas of anomalous concentration of potentially hazardous elements by means of a subcatchment-based discriminant analysis of stream sediments. *Journal of Geochemical Exploration*, *87*(3), 83-91.

Sun, X., Zheng, Y., Wang, C., Zhao, Z., & Geng, X. (2016). Identifying geochemical anomalies associated with Sb–Au–Pb–Zn–Ag mineralization in north Himalaya, southern Tibet. *Ore Geology Reviews*, *73*, 1-12.

Thompson, M., & Howarth, R. J. (1978). A new approach to the estimation of analytical precision. *Journal of Geochemical Exploration*, *9*(1), 23-30.

Tukey, JW. (1977). *Exploratory data analysis* (2). Addison-Wesley. Retrieved October 27, 2021, from https://onlinelibrary.wiley.com/doi/abs/10.1002/bimj.4710230408.

Wang, W., Cheng, Q., Zhang, S., & Zhao, J. (2018). Anisotropic singularity: A novel way to characterize controlling effects of geological processes on mineralization. *Journal of Geochemical Exploration*, *189*, 32-41.

Wang, W., Zhao, J., & Cheng, Q. (2011). Analysis and integration of geo-information to identify granitic intrusions as exploration targets in southeastern Yunnan District, China. *Computers & Geosciences*, *37*(12), 1946-1957.

Yilmaz, H. (2003). Geochemical exploration for gold in western Turkey: success and failure. *Journal of Geochemical Exploration*, *80*(1), 117-135.

Yilmaz, H., Yousefi, M., Parsa, M., Sonmez, F. N., & Maghsoodi, A. (2019). Singularity mapping of bulk leach extractable gold and− 80# stream sediment geochemical data in recognition of gold and base metal mineralization footprints in Biga Peninsula South, Turkey. *Journal of African Earth Sciences*, *153*, 156-172.

Yousefi, M. (2017a). Analysis of zoning pattern of geochemical indicators for targeting of porphyry-Cu mineralization: a pixel-based mapping approach. *Natural Resources Research*, *26*(4), 429-441.

Yousefi, M. (2017b). Recognition of an enhanced multi-element geochemical signature of porphyry copper deposits for vectoring into mineralized zones and delimiting exploration targets in Jiroft area, SE Iran. *Ore Geology Reviews*, *83*, 200-214.

Yuan, F., Li, X., Zhou, T., Deng, Y., Zhang, D., Xu, C., ... & Jowitt, S. M. (2015). Multifractal modelling-based mapping and identification of geochemical anomalies associated with Cu and Au mineralisation in the NW Junggar area of northern Xinjiang Province, China. *Journal of Geochemical Exploration*, *154*, 252-264.

Zuo, R. (2011). Identifying geochemical anomalies associated with Cu and Pb–Zn skarn mineralization using principal component analysis and spectrum–area fractal modeling in the Gangdese Belt, Tibet (China). *Journal of Geochemical Exploration*, *111*(1-2), 13-22.

Zuo, R., & Wang, J. (2016). Fractal/multifractal modeling of geochemical data: A review. *Journal of Geochemical Exploration*, *164*, 33-41.

Zuo, R., Xia, Q., & Wang, H. (2013). Compositional data analysis in the study of integrated geochemical anomalies associated with mineralization. *Applied geochemistry*, *28*, 202-211.

Zuo R., Xia Q., & Zhang D., (2013). A comparative study of the C-A and S-A models with singularity analysis to identify geochemical anomalies in covered areas. *Applied Geochemistry 33*,165–172.